Mutagenic, Electrochemical, and Crystallographic Investigation of the Cytochrome b_5 Oxidation-Reduction Equilibrium: Involvement of Asparagine-57, Serine-64, and Heme Propionate-7[†,‡]

Walter D. Funk,[§] Terence P. Lo,[∥] Marcia R. Mauk, Gary D. Brayer,* Ross T. A. MacGillivray,* and A. Grant Mauk*

Department of Biochemistry, University of British Columbia, Vancouver, British Columbia V6T 1W5, Canada
Received December 14, 1989; Revised Manuscript Received February 8, 1990

ABSTRACT: A gene coding for lipase-solubilized bovine liver microsomal cytochrome b_5 has been synthesized, expressed in *Escherichia coli*, and mutated at functionally critical residues. Characterization of the recombinant protein revealed that it has a reduction potential that is approximately 17 mV lower than that of authentic wild-type protein at pH 7 (25 °C). Structural studies determined that the recombinant protein differed in sequence from authentic wild-type cytochrome b_5 owing to three errors in amidation status in the published sequence for the protein on which the gene synthesis was based. The structural origin of the lower reduction potential exhibited by the triple mutant has been investigated through X-ray crystallographic determination of the three-dimensional structure of this protein and is attributed to the presence of Asp-57 within 3.3 Å of heme vinyl-4 in the mutant. In addition, the model developed by Argos and Mathews [Argos, P., & Mathews, F. S. (1975) *J. Biol. Chem. 250*, 747] for the change in cytochrome b_5 oxidation state has been studied through mutation of Ser-64 to Ala. In this model, Ser-64 is postulated to stabilize the oxidized protein through H-bonding interactions with heme propionate-7 that orients this propionate group 6.2 Å from the heme iron. Spectroelectrochemical studies of a mutant in which Ser-64 has been changed to an alanyl residue demonstrate that this protein has a reduction potential that is 7 mV lower than that of the wild-type protein; moreover, conversion of the heme propionate groups to the corresponding methyl esters increases the potential by 67 mV. These results establish that elimination of one of the hydrogen bonds formed between Ser-64 and heme propionate-7 in ferricytochrome b_5 is not sufficient to destabilize this form of the protein. We conclude that the increase in reduction potential produced by heme propionate esterification results from elimination of a carboxylate inductive effect or simply from removal of two negatively charged functional groups that are in proximity to the heme group.

The conformational alterations that accompany the change in oxidation state of electron-transfer proteins are major contributing factors to the rates of electron transfer exhibited by such proteins and to the relative stabilities of the oxidized and reduced forms (i.e., the reduction potentials) of such proteins. The most detailed models for redox-linked conformational changes of electron-transfer proteins have arisen from crystallographic analysis of the reduced and oxidized forms of cytochrome *c* (Takano & Dickerson, 1981a,b; Louie et al., 1988a,b) and lipase-solubilized, bovine liver microsomal cytochrome b_5 (Argos & Mathews, 1975). In the case of cytochrome b_5, Argos and Mathews (1975) have proposed that hydrogen bonds formed between the main-chain amide and side-chain hydroxyl group of Ser-64 and the two carboxylate oxygen atoms of heme propionate-7 (Mathews, 1980) result in an orientation of this heme propionate that stabilizes the net positive charge on the heme iron of ferricytochrome b_5 through Coulombic interaction. In ferrocytochrome b_5, a cation was suggested to interact with heme propionate-7 (Argos & Mathews, 1975) without any change in orientation of this group.

In an attempt to perturb the orientation of heme propionate-7, destabilize ferricytochrome b_5, and thereby increase the reduction potential of the protein, we have constructed a mutant of cytochrome b_5 in which Ser-64 is replaced by an alanyl residue. This undertaking has been achieved through the construction of a synthetic gene coding for the lipase-solubilized, bovine liver microsomal form of cytochrome b_5 and its expression in *Escherichia coli*. In the course of this work, we have also determined that the reported amino acid sequence for bovine liver microsomal cytochrome b_5 is incorrect at three positions and have demonstrated that these sequence errors have a significant, unanticipated effect on the electrochemical properties of this protein. To assess the structural basis for these functional alterations, the three-dimensional structure of the triple mutant has been determined by X-ray crystallographic techniques.

Experimental Procedures

Materials. The large fragment (Klenow) of *E. coli* DNA polymerase I, T4 DNA ligase, polynucleotide kinase, and all restriction enzymes were purchased from Bethesda Research Laboratories. Deoxy- and dideoxynucleoside triphosphates were obtained from Pharmacia, and [α-^{32}P]dATP was obtained from Amersham. Hen egg white lysozyme, deoxy-

[†] This work was supported by MRC Operating Grants MT-7182 (to A.G.M.), MA-7975 (to G.D.B.), and MT-10317 (to R.T.A.M.). The FPLC system was obtained through a grant from the British Columbia Health Care Research Foundation (to A.G.M.).

[‡] The nucleic acid sequence in this paper has been submitted to GenBank under Accession Number J02905.

[§] Recipient of a studentship from the Medical Research Council of Canada Biotechnology Training Program at the University of British Columbia (1986-1988).

[∥] Recipient of a studentship from the Medical Research Council of Canada.

0006-2960/90/0429-5500$02.50/0

ribonuclease I, and ribonuclease A were purchased from Sigma. Poly(ethylene glycol) 4000 (PEG) was from BDH Chemicals. Ferriprotoporphyrin IX dimethyl ester was obtained from Porphyrin Products, Logan, UT. $Ru(NH_3)_6Cl_3$ (Alfa) was purified as described by Pladziewicz et al. (1973). All other chemicals were reagent grade or better.

Gene Construction. Oligodeoxyribonucleotides (designated B1–B4) were synthesized on an Applied Biosystems 380A DNA synthesizer and were purified by polyacrylamide gel electrophoresis under denaturing conditions, followed by reverse-phase liquid chromatography with a Sep-Pak C_{18} cartridge (Waters Associates) (Atkinson & Smith, 1984). The 5′ ends of the oligonucleotides were subsequently phosphorylated with T4 polynucleotide kinase and ATP (Chaconas & van de Sande, 1980). Equimolar amounts of oligonucleotides with overlapping 3′ ends were then combined with the Klenow fragment of DNA polymerase I and dNTPs. The resulting blunt-ended, double-stranded DNA was then cloned into the *Sma*I site of phage M13mp18 (Messing, 1983). The fidelity of the DNA synthesis step was confirmed by DNA sequence analysis using the chain termination method (Sanger et al., 1977). A *Bam*HI/*Hha*I fragment corresponding to the sequence covered by oligonucleotides B1 and B2 and a *Hha*I/*Eco*RI fragment covering the B3 and B4 sequence were then excised from the appropriate M13 RF DNA and ligated into *Bam*HI/*Eco*RI-cut pUC19 (Messing, 1983), followed by transformation into *E. coli* JM83. Clones were analyzed by restriction mapping. The complete nucleotide sequence of the final gene construct was determined for both strands.

Protein Purification. Bacteria transformed with pUC-cyt b_5 plasmid were grown for 16 h (37 °C) in YT medium (4 L) containing ampicillin (50 mg/L). This inoculum was used to seed a 50 L culture of the same medium. The bacteria were allowed to grow at 37 °C with vigorous aeration to stationary phase (ca. 4–6 h). At this point, the aeration was decreased to a minimal level, and the culture was incubated for a further 20 h. This latter step improved the yield of cytochrome, presumably by permitting sufficient heme synthesis to accommodate the apocytochrome b_5 produced (S. G. Sligar, personal communication). Bacteria were harvested with a continuous centrifuge (New Brunswick Model 43), and the cell paste was resuspended in 1 L of lysis buffer as described (von Bodman et al., 1986). Following a 1-h incubation at 37 °C, the lysis was completed by a single pass through a French press (1200 psi), and the cell debris was removed by centrifugation at 8600*g* for 30 min (4 °C). KCl and PEG (final concentrations 0.4 M and 6%, respectively) were added to the supernatant solution. This solution was stirred for 15 min and then centrifuged at 8600*g* for 30 min (4 °C). This supernatant solution was brought to 50% $(NH_4)_2SO_4$ saturation, stirred at 4 °C for 1 h, and then centrifuged at 8600*g* (4 °C). The resulting supernatant solution was dialyzed exhaustively against water until the conductivity equaled that of sodium phosphate buffer (20 mM, pH 7.2). The dialyzate was clarified by centrifugation at 8600*g*, loaded onto a column (2.5 × 12 cm) of DE-52 cellulose (Whatman), washed with one column volume of 50 mM sodium phosphate buffer (pH 7.2), and eluted with 150 mM sodium phosphate buffer (pH 7.2). Fractions containing cytochrome b_5 were identified by their red color, concentrated by ultrafiltration (Amicon YM-5 membrane or Centriprep-10), and exchanged into 20 mM triethanolamine (pH 7.3). The cytochrome was further purified by chromatography on an HR 10/10 Mono-Q FPLC column (Pharmacia) in 20 mM triethanolamine (pH 7.3) with a linear gradient of 0.2–0.29 M NaCl. Fractions containing protein with an $A_{412.5}/A_{280}$ ratio of ≥5.9 were pooled, concentrated by ultrafiltration, and stored in liquid nitrogen. Replacement of the native protoheme IX prosthetic group with heme IX dimethyl ester was performed as described previously (Reid et al., 1984).

Tryptic Peptide Mapping. Apocytochrome b_5 was prepared by the method of Teale (1959; Reid et al., 1984). One milligram of the apoprotein was digested in 0.5 mL of 0.2 M NH_4HCO_3 with 12.5 μL of a stock solution of L-1-(tosylamino)-2-phenylethyl chloromethyl ketone (TPCK-) trypsin (Worthington, Cooper Diagnostics) (1.0 mg/mL TPCK-trypsin in 1 mM HCl) at 37 °C for 6 h. An additional 12.5 μL of the TPCK-trypsin solution was then added, and the digestion was continued for a further 18 h. After addition of 100 μL of 1 M HCl, the sample was lyophilized, and the hydrolysis procedure was repeated. The final lyophilized pellet was dissolved in 1.0 mL of 0.05% TFA. Reverse-phase HPLC tryptic peptide maps were developed from 100-μL samples of this digest with a Varian Model 5060 HPLC system equipped with a Vista 401 data station and fitted with an Alltech C_{18} reverse-phase column (4.6 × 250 mm). Peptides were eluted with a gradient of acetonitrile (0–60%) in 0.05% TFA, over 135 min at a flow rate of 1.0 mL/min.

Amino Acid Sequence Analysis. The amino-terminal sequence of recombinant lipase-solubilized cytochrome b_5 and the total sequences of selected tryptic peptides obtained from HPLC maps of the recombinant lipase-solubilized protein and authentic trypsin-solubilized bovine liver cytochrome b_5 were determined on 1-nmol samples of each. Vapor-phase amino acid sequence analysis was performed with an Applied Biosystems 477A protein sequencer by the Protein Microchemistry Centre at the University of Victoria (tryptic peptides) or by Prof. Ian Clark-Lewis at the Biomedical Research Centre at the University of British Columbia.

Limited Tryptic Hydrolysis. Tryptic hydrolysis to convert the recombinant lipase-solubilized cytochrome b_5 to the trypsin-solubilized form was performed by the method of Strittmatter and Ozols (1966). Tryptic hydrolysates were chromatographed on a Mono-Q column (HR 5/5) (Pharmacia) in 20 mM triethanolamine (pH 7.3) with a linear gradient of 0.19–0.32 M NaCl.

Site-Directed Mutagenesis. All modifications to the synthetic gene coding for cytochrome b_5 were accomplished by the method of Zoller and Smith (1983) using the *dut*⁻, *ung*⁻ selection procedure (Kunkel, 1985).

Spectroelectrochemistry. Potentiometric titrations were performed with an optically transparent thin-layer electrode (OTTLE) described previously (Reid et al., 1982; Reid, 1984) with $Ru(NH_3)_6Cl_3$ used as a mediator. Solution potentials were measured against the saturated calomel electrode (Radiometer K4112) (SCE) and converted to the hydrogen scale as described by Dutton (1978).

Three-Dimensional Structure Determination. Small crystals of the triple mutant of recombinant bovine lipase solubilized ferricytochrome b_5 were grown by the hanging drop vapor diffusion method under conditions similar to those employed for crystallization of the wild-type protein (Mathews & Strittmatter, 1969). Larger, diffraction-quality crystals were obtained by hair seeding hanging drops containing 3 mg/mL protein and 2.6 M phosphate buffer (pH 7.1) (Leung et al., 1989). These drops of protein solution were equilibrated against a 1-mL reservoir containing 3.2 M phosphate buffer. All crystallizations were conducted at room temperature (21 °C).

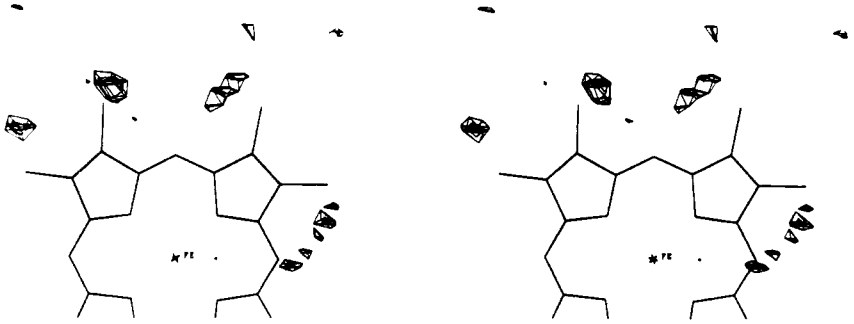

FIGURE 1: Difference Fourier synthesis after refinement with heme vinyl methylene carbons deleted from the model of the triple-mutant cytochrome. This map shows four distinct positions for vinyl methylene carbons, one pair of peaks for each of two possible rotational orientations of the heme. The difference peaks observed are the highest features in the vicinity of the heme moiety. The contour levels drawn represent 0.17 e/Å^3 (2.5σ) and 0.19 e/Å^3 (2.8σ).

When equilibrated at 15 °C for diffraction data collection, these crystals proved to be unstable if kept in phosphate buffers having a concentration ranging between 3.2 and 3.5 M and a pH ranging from 7.1 to 7.5. Such increased solubility at lower temperatures is common for proteins in high ionic strength buffers (Jakoby, 1971; McPherson, 1982). Therefore, crystals were soaked in 4.0 M phosphate buffer before being mounted in thin-walled glass capillaries for diffraction analyses. Crystals prepared in this manner proved to be stable at 15 °C for periods of over 1 month. From precession photography, the space group of these crystals was determined to be $P6_2$ (or its enantiomorph $P6_4$). Unit-cell parameters were found to be $a = b = 63.94$ (2) Å and $c = 39.67$ (2) Å on the basis of diffractometer measurements and the least-squares centering of 25 orientation reflections.

A complete set of X-ray diffraction intensities to 1.9-Å resolution was collected from a single crystal measuring 0.5 × 0.35 × 0.35 mm on an Enraf-Nonius CAD4-F11 diffractometer equipped with a helium-filled beam tunnel and having a crystal to counter distance of 36.8 cm. The incident radiation was nickel filtered and generated from a copper-target X-ray tube (0.75 mm × 15 mm focal spot) operated at 26 mA and 40 kV. Continuous ω scans of width 0.6° were used to collect intensities, with the initial and final one-sixth of the scan taken as a measure of background intensity. Three high-intensity reflections were used to monitor crystal decay and slippage and were measured every 2.8 h of X-ray exposure time. At the end of the data collection, these three monitor reflections had decayed by approximately 28%.

Intensity data were corrected for backgrounds, absorption (North et al., 1968), and crystal decay, following which the 11 716 measurements were merged to a unique set of 7460 reflections with a merging R factor of 7.4%. This merged data set was then corrected for Lorentz and polarization effects and converted to structure factor amplitudes. These data were placed on an absolute scale according to the method of Thiessen and Levy (1973), which employs a least-squares variant of the Wilson (1942) plot statistical method. The overall isotropic temperature factor was estimated to be 17.6 Å^2. A molecular replacement approach was taken to solving the phase problem, the 2.0 Å resolution structure of wild-type cytochrome b_5 (Mathews et al., 1972) being used as a starting model. Solution of both the rotation and translation functions used the MERLOT software package (Fitzgerald, 1988). Application of the translation function in both enantiomorphic space groups indicated a single unique solution and confirmed the space group to be $P6_2$. Rotational and translational parameters were then optimized with the program BRUTE (Fujinaga & Read, 1987). This procedure resulted in a sharp peak with a correlation coefficient of 55.4% and an R factor of 47.7% for the 699 reflections falling in the 8.0–4.0-Å resolution range with $F \geq 1\sigma(F)$.

All subsequent structural refinement employed a restrained parameter least-squares procedure (Hendrickson & Konnert, 1981) at increasing ranges of data resolution. Manual revisions were made at several points in the refinement process on the basis of the systematic inspection of $F_o - F_c$, $2F_o - F_c$, and $3F_o - 2F_c$ difference electron density maps sequentially covering the entire course of the polypeptide chain. The majority of refitting involved the placement of additional residues at both termini (residues 1, 2, and 88–93), which were missing from the original wild-type cytochrome b_5 structure (Mathews et al., 1971, 1972; Mathews, 1985) and are relatively poorly resolved in the present structure. A total of 65 water molecules was also added to the refinement model during manual inspections. A conservative approach was taken in assigning water molecule positions, requiring that these be at least 2.8 Å from the protein surface and be fully occupied as judged by the magnitudes of electron density peaks assigned to nearby polypeptide chains. Water molecules were refined as neutral oxygen atoms with individual temperature factors and occupancies set to 1.0.

To evaluate the possibility of multiple heme orientations (having alternative vinyl positions) within the mutant protein, both vinyl methylene carbons were removed after refinement cycle 155, and the remaining structure was refined for three cycles. Examination of a subsequent $F_o - F_c$ difference electron density map clearly showed an ambiguity in vinyl positioning as illustrated in Figure 1. Structure refinement was continued with the most highly populated heme orientation, which also had the optimal heme vinyl steric contacts (see Results).

Following a total of 169 cycles of refinement (individual isotropic B values were used after cycle 20), the final standard crystallographic R factor was 15.1% for the 4751 structure factors [with $F \geq 3\sigma(F)$] in the resolution range 6.0–1.9 Å. In addition to refining well against the observed diffraction data, the current structural determination has good stereochemistry. A listing of these geometric parameters and the refinement restraint weighting values used in the final cycle of refinement is presented in Table I.

RESULTS

Gene Design and Synthesis. Overlapping oligonucleotides were designed to allow the second strand of the DNA to be synthesized enzymatically with DNA polymerase I (Figure 2a). The resulting blunt-ended fragments contained internal *Kpn*I, *Hha*I, and *Eco*RI restriction enzyme recognition sequences, which were used to assemble the final construct into plasmid pUC 19. The gene cassette (Figure 2b) utilizes a transcriptional fusion strategy with the lacZ transcript and

Table I: Stereochemistry of Recombinant Bovine Lipase-Solubilized Cytochrome b_5 Triple Mutant

stereochemical refinement parameter	rms deviation from ideal values	refinement restraint weighting values
bond distances (Å)	0.020	0.018
angle distances (Å)	0.043	0.030
planar 1–4 distances (Å)	0.055	0.045
planes (Å)	0.017	0.018
chiral volumes (Å^3)	0.183	0.120
ω bond angles (deg)	2.5	2.5
nonbonded contact (Å)[a]		
single torsion	0.240	0.300
multiple torsion	0.241	0.300
possible H-bond	0.237	0.300

[a] The rms deviations from ideality for this class of restraint incorporate a reduction of 0.2 Å from the radius of each atom involved in a contact.

includes an in-frame translational stop codon followed immediately by a Shine–Delgarno site. The spacer region between the ribosome binding site and the initiator methionine was modeled on the *Pseudomonas* cytochrome P-450$_{cam}$ sequence, which has been used successfully in the expression of rat liver cytochrome b_5 in *E. coli* (von Bodman et al., 1986). This region was modified to conform to consensus base rules for this region (Scherer et al., 1980; Stormo et al., 1982), by shortening the distance between the ribosome binding site and initiator methionine to nine base pairs. Codons were chosen to reflect the *E. coli* bias (Maruyama et al., 1986).

Protein Expression and Purification. Transformation of *E. coli* JM 83 with the gene coding for the lipase-solubilized form of cytochrome b_5 resulted in high levels of recombinant protein in the bacteria. NaDodSO$_4$–PAGE analysis of whole cell lysates showed cytochrome b_5 as constituting up to 15% of the total cellular protein as judged by optical density scanning (data not shown). We routinely obtain 500 mg of purified protein from 50-L fermentation cultures; however, this represents only about 10% of the expected yield based on the above gel analysis, assuming 15% of the wet weight of *E. coli* as protein (Lehninger, 1970). The reason for this discrepancy is unclear, though it may reflect the inability of the host to supply sufficient heme for the cytochrome load combined with instability of apocytochrome b_5 to the conditions of protein isolation. Attempts at reconstituting cell lysates with exogenous heme have not been productive. Alternatively, this discrepancy may arise from anomalous staining of cytochrome b_5 in the NaDodSO$_4$–PAGE analysis of *E. coli* proteins.

Amino-Terminal Sequence Analysis. Gas-phase protein sequencing of the amino-terminal region of the recombinant cytochrome showed complete agreement with the predicted sequence from DNA analysis (Figure 2b). The absence of a peptide containing formylmethionine in the tryptic peptide maps (vide infra) indicates complete processing of the amino terminus as has been reported for the recombinant rat liver cytochrome b_5 species (von Bodman et al., 1986).

Tryptic Peptide Mapping. Our initial peptide mapping of the recombinant cytochrome indicated that all predicted tryptic fragments were present. Within the resolution of the process, the HPLC retention times of these peptides appeared to match those of peptides produced from authentic trypsin-solubilized bovine liver cytochrome b_5 that had been purified by the method of Reid and Mauk (1982). Additional peptides in the profile of the recombinant sample were predicted to result from the amino- and carboxyl-terminal extensions of the lipase-solubilized recombinant form versus the trypsin-solubilized bovine liver cytochrome b_5. Amino acid composition analysis

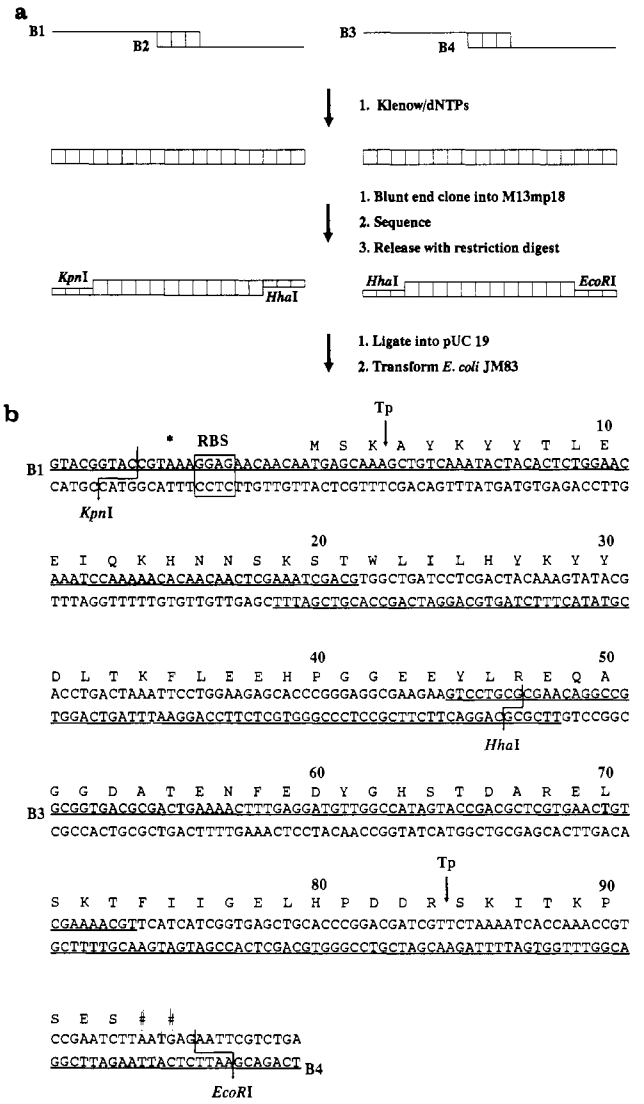

FIGURE 2: (a) Assembly strategy for the recombinant lipase-solubilized, bovine microsomal cytochrome b_5. Two pairs of overlapping oligonucleotides (B1–B4) were filled in with Pol 1, sequenced in m13mp18, released with restriction digests, and assembled into pUC 19. (b) Nucleotide sequence of the gene construct for wild-type, lipase-solubilized bovine liver microsomal cytochrome b_5. Overlapping oligonucleotides used in assembling the gene are underlined. The ribosome binding site (RBS) is indicated by boxed nucleotides, and restriction endonuclease cleavage sites relevent to the gene assembly are noted by arrows. An in-frame stop codon for the lacZ transcript and translation termination codons for the cytochrome are denoted by (*) and (#), respectively. The sites of cleavage by trypsin that produce the core heme-binding domain are denoted by Tp.

of these additional peptides confirmed this expectation.

FPLC Analysis of Authentic and Recombinant Cytochromes b_5. On the basis of inequivalent electrochemical (vide infra), chromatographic, cytochrome *c* binding, and methemoglobin binding behavior (Mauk, Funk, MacGillivray, and Mauk, unpublished) and NMR (Burch et al., 1990) properties of the recombinant and authentic cytochromes, we extended our analysis in two ways to assure that the sequences of the two proteins were identical for the 82 residues that are common to both. First, we compared the chromatographic behavior of the recombinant and authentic cytochromes by FPLC. In this experiment, we converted the recombinant protein (with the "lipase-solubilized" sequence) to the corresponding tryptic form by mild hydrolysis with TPCK-trypsin (Strittmatter & Ozols, 1966). FPLC analysis of the products revealed three species, none of which exhibited elution behavior identical with

Table II: Reduction Potentials of Recombinant Bovine Liver Microsomal Cytochrome b_5 Derivatives

protein	prosthetic group	$E_{m,7}$ (mV vs SHE)[a]	Nernst slope (mV)
wild type (correct sequence)	protoheme IX	3	57.9
	protoheme IX DME	70	61.2
Ala-64 (correct sequence)	protoheme IX	−4	59.0
	protoheme IX DME	63	56.9
triple mutant	protoheme IX	−14	59.0
triple mutant with Ala-64	protoheme IX	−19	62.0

[a] 25 °C, sodium phosphate (μ = 0.1 M).

that of authentic trypsin-solublized cytochrome b_5 (data not shown). The major tryptic product generated from the recombinant protein exhibited a prolonged retention time relative to the authentic sample, indicating that it is more anionic in nature. Second, we prepared multiple tryptic peptide maps of both recombinant and authentic cytochrome to evaluate the uncertainty of tryptic peptide retention times. This experiment demonstrated slight but reproducible differences in the retention times of peptides T2 and T7 produced from the two proteins. Gas-phase sequence analysis of these peptides revealed that the peptides from authentic cytochrome b_5 possessed the amino acid sequence predicted from the work of Cristiano and Steggles (1989) while the peptides from the recombinant cytochrome were identical with the target sequence of Ozols and Strittmatter (1969) and differed from the Cristiano and Steggles sequence in the amidation status of three residues. The corrected assignments are as follows: Asn-57, Gln-13, and Glu-11. In light of the report by Cristiano and Steggles (1989) and the recent revision of the bovine cytochrome b_5 sequence by Ozols (1989), the details of our results are not elaborated here.

Site-Specific Mutagenesis and Amino-Terminal Sequence Analysis. Two oligonucleotides spanning the sequence for residues 11 and 13 and for residue 57 were produced to alter the synthetic gene so that it would code for the correct wild-type sequence. While the corrected wild-type, recombinant lipase-solubilized cytochrome b_5 could still be distinguished from authentic trypsin-solubilized cytochrome, the tryptic fragment derived from the lipase-solubilized cytochrome now eluted at the same point in the gradient as the authentic sample, thereby confirming the identity of the corrected recombinant protein and the authentic material (data not shown).

Spectroelectrochemical Studies. The results of potentiometric titrations performed with the thin-layer cell are illustrated for both the corrected wild-type protein and the corresponding Ala-64 mutant in Figure 3. Both proteins exhibited electrochemically reversible behavior as observed previously for protein isolated from liver (Reid et al., 1982). The midpoint potentials and Nernst slopes obtained for wild-type cytochrome b_5 possessing the correct and incorrect amino acid sequence are shown in Table II. Notably, the midpoint potential for recombinant lipase-solubilized cytochrome b_5 is essentially identical with the value that we have previously reported for trypsin-solubilized cytochrome b_5 isolated from liver (Reid et al., 1982). On the other hand, the potential of the recombinant protein possessing the incorrect sequence exhibits a reduction potential that is 17 mV lower than that of the true wild-type protein.

As previously observed for trypsin-solubilized cytochrome b_5 isolated from liver, the replacement of the native protoheme IX prosthetic group with protoheme IX dimethyl ester increases the reduction potential of wild-type lipase-solubilized

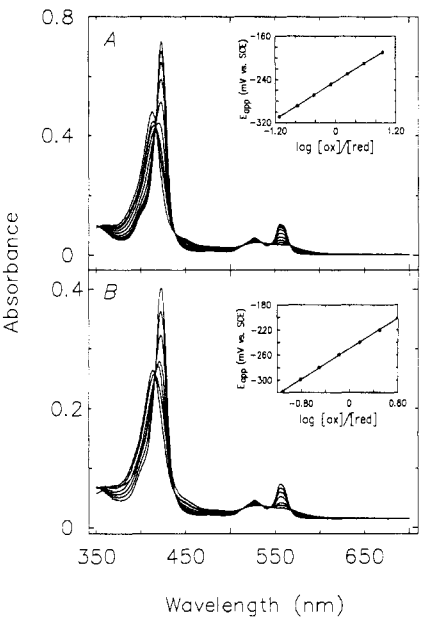

FIGURE 3: Thin-layer spectra of wild-type and mutant forms of recombinant, lipase-solubilized bovine liver microsomal cytochrome b_5. Cytochrome b_5 (120 μM), $Ru(NH_3)_6^{2+/3+}$ (12 μM), 25 °C, pH 7.0 (phosphate), μ = 0.1 M. The spectra were collected over a potential range of −320 to + 50 mV vs SCE. The inserts represent Nernst plots derived from the absorbance reading at 423.5 nm. (a) Wild-type, recombinant lipase-solubilized, bovine liver microsomal cytochrome b_5; (b) the Ala-64 mutant of the protein shown in (a).

cytochrome b_5 by 67 mV (Table II). Interestingly, the same increase in potential is observed when the same modification is introduced into the Ala-64 mutant (Table II).

Three-Dimensional Structure of the Cytochrome b_5 Triple Mutant. The general features of the structural model for the cytochrome b_5 triple mutant correspond closely to those of the wild-type protein (Mathews et al., 1971; Durley and Mathews, unpublished results) as illustrated in the stereo diagram of the α-carbon backbones of the two proteins shown in Figure 4. The similarity of these two structures is described quantitatively by the plot of average deviations in the positions of the main-chain and side-chain atoms provided in Figure 5. No refolding of the polypeptide main chain has occurred at any of the mutated sites, although the side chain of residue 11 has shifted significantly as seen in Figure 6. In the wild-type protein, the carboxyl group of Glu-11 forms electrostatic interactions with the side chains of both Lys-14 and His-15. In the mutant protein, the side chain of Gln-11 rotates and forms H-bonds to the hydroxyl group and main-chain nitrogen of Thr-8. In both proteins, the His-15 imidazole forms a H-bond to the side-chain hydroxyl group of Ser-20.

Mutation of Asn-57 to Asp introduces an additional negative charge in close proximity to the prosthetic heme group. In the wild-type structure, the γ-carbon of Asn-57 is 10.1 Å from the heme iron atom, and in the mutant, this distance increases to 11.3 Å. Nevertheless, the side chain of Asp-57 remains sufficiently close to the heme group to influence the electrochemical behavior of the protein because the β-carbon of Asp-57 is just 3.3 Å from the methylene carbon atom of the 4-vinyl group. The proximity of these two moieties may facilitate the relative stabilization of ferricytochrome b_5 through an electronic inductive effect permitted through conjugation of the 4-vinyl group to the π-system of the porphyrin ring.

The amino and carboxyl termini of the triple mutant are not well ordered as can be seen from the plot of isotropic thermal parameters provided in Figure 7. The *B* values of the residues at both ends of the protein are well above the

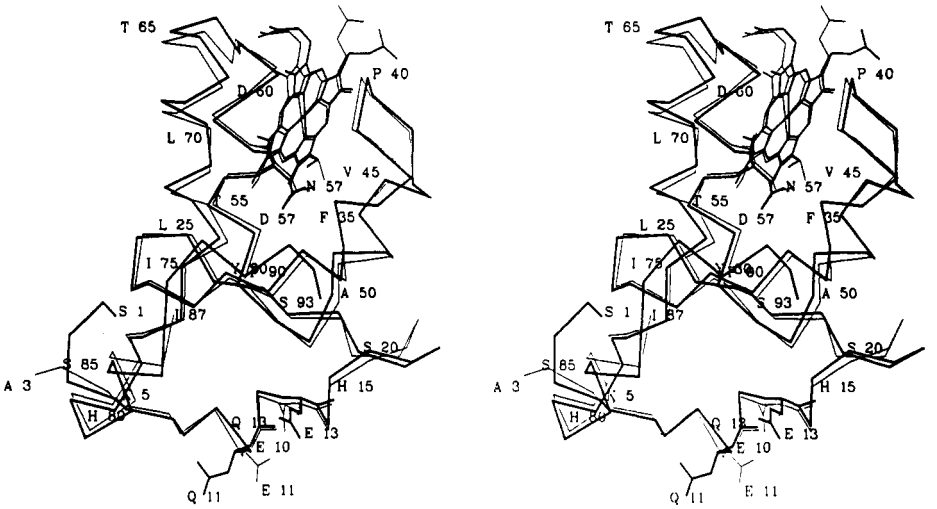

FIGURE 4: Stereo diagram showing an overlap of the α-carbon backbone and heme group of the wild-type cytochrome b_5 structure (thin lines) and the triple-mutant structure (thick lines). The two structures were aligned by a least-squares fit of common main-chain atoms. The α-carbon atom of every fifth residue has been labeled with its one-letter amino acid designation and sequence number (see Figure 2b). Side-chain atoms at the three sites of mutation (residues 11, 13, and 57) have also been drawn.

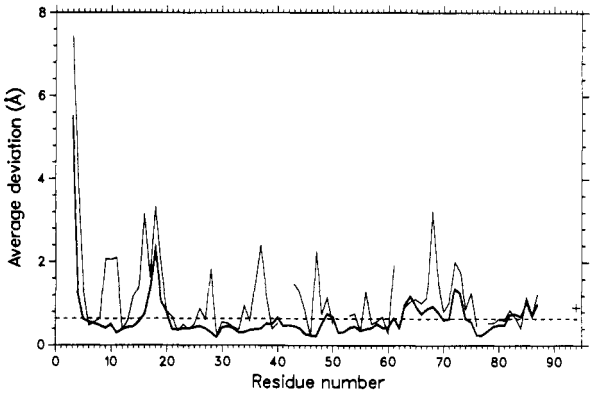

FIGURE 5: Plot of the average positional deviations between corresponding main-chain atoms (thick line) and side-chain atoms (thin line) in wild-type and triple-mutant lipase-solubilized bovine liver cytochrome b_5. No side-chain deviation value is plotted for glycine residues. The overall average deviation of heme atoms is represented as a (+) at position 94. The average deviation between all common main-chain atoms is 0.65 Å and is represented by the dashed line.

average B value of 18.6 Å^2 found for the protein as a whole. Nevertheless, the current results permit extension of the structural model to include the amino-terminal Ser and penultimate Lys residues that could not be identified in the electron density data collected for the wild-type protein. Similarly at the carboxyl terminus, residues 88–93 which were not identified in the wild-type structure were observed and have been added into the current structural model. Large solvent channels exist in the area of both terminal regions in the hexagonal crystals studied here.

The dominant orientation of the heme in the triple-mutant protein is the same orientation found to exist in the wild-type lipase-solubilized protein by NMR techniques (Keller & Wüthrich, 1980) and by X-ray diffraction techniques (Mathews, 1980). From the heme vinyl methylene carbon fragment deleted difference electron density map (Figure 1), we estimate that roughly 60% of the crystalline triple-mutant cytochrome exhibits the dominant heme orientation and 40% exhibits the alternate orientation. In the dominant orientation, the 4-vinyl group exhibits rotational disorder about the C3C–CAC bond while in the alternate orientation, steric constraints prevent this rotation. This observation provides a structural explanation for the preference the protein exhibits for the dominant orientation and is consistent with NMR studies of La Mar et al. (1984) concerning the involvement of heme substituents in determining the heme disorder equilibrium in heme binding to sperm whale myoglobin.

The heme environment in the triple mutant (dominant heme orientation) exhibits relatively subtle differences in comparison with that in the wild-type protein (dominant orientation). For example, the solvent-accessible surfaces (Connolly, 1983) of the heme groups in the two proteins are similar. In both proteins, the heme iron atom is octahedrally coordinated with no ligand distance deviating more than 0.06 Å from 2.00 Å in either structure. However, by fitting the structures of the wild-type and mutant cytochromes to each other, a small distortion of the axial ligand geometry can be observed in the mutant structure (Figure 8). Specifically, the angle formed by the normal to the least-squares plane of the His-63 imidazole ring and the normal to the least-squares heme plane

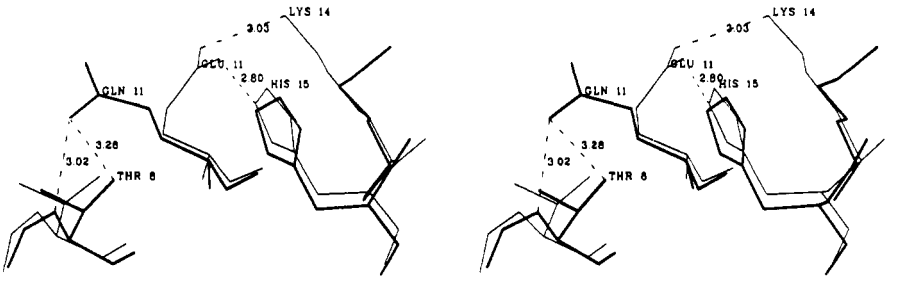

FIGURE 6: Hydrogen bonding of residue 11 in the wild-type structure (thin lines) and the triple-mutant structure (thick lines). Interactions between Glu-11 and residues 14 and 15 in the wild-type structure and between Gln-11 and residue 8 in the mutant structure are indicated by dashed lines and hydrogen-bond lengths.

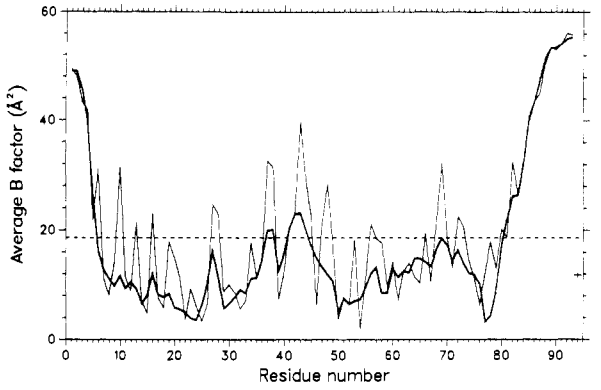

FIGURE 7: Plot of average isotropic thermal parameters for main-chain atoms (thick lines) and side-chain atoms (thin lines) by residue number for the cytochrome b_5 triple mutant. The average heme *B* factor of 11.8 Å^2 is indicated by a (+) at position 94, and the average *B* factor for the protein of 18.6 Å^2 is indicated by the horizontal dashed line.

changes from 84.8° in the wild-type structure to 95.2°. In addition, the angle formed by the normals to the least-squares planes of the His-63 and His-39 imidazole ring systems is 20.8° in the wild-type protein and 25.2° in the mutant.

The H-bonds formed by heme propionate-7 with the Ser-64 amide nitrogen, Ser-64 hydroxyl group, and a water molecule are geometrically similar and have similar bond lengths in both structures. Although heme propionate-6 adopts different conformations in the two structures (Figure 8), in each case this group is fully solvated and forms no H-bonds or electrostatic interactions with protein atoms. The 2-vinyl and 4-vinyl groups in the wild-type structure assume different angles with respect to the least-squares heme plane than those in the mutant cytochrome; however, ambiguity in the exact positions of the vinyl groups in the mutant structure precludes quantitative comparisons.

The largest structural difference between the mutant and wild-type structures occurs in the vicinity of Ser-18, a region of the protein some distance from the sites of mutation. Aside from the amino- and carboxyl-terminal regions of the protein discussed above, the peptide loop containing residues 17–19 exhibits the greatest positional difference between the wild-type and mutant structures (Figure 5). In particular, the main-chain atoms of Ser-18 have an average deviation of over 2.0 Å between the two structures. Interestingly, the thermal *B* factors for the loop containing residues 17–19 are relatively high in the refined wild-type structure (Durley and Mathews, unpublished results), indicating that this loop is quite flexible. As seen in Figure 7, the thermal factors in the 17–19 loop range between 5.3 and 11.1 Å^2 for the main-chain atoms and between 4.2 and 23.6 Å^2 for side-chain atoms in the triple-mutant structure, indicating that this region of the protein is well ordered. The origin of this greater order in the hexagonal crystalline form is probably attributable to an intermolecular H-bond that forms between heme propionate-7 and Ser-18 of symmetry-related molecules. In other words, in the mutant structure, packing against a symmetry-related cytochrome b_5 molecule has stabilized the flexible 17–19 loop in an alternate conformation.

Discussion

As pioneered by Sligar and co-workers in their work with both cytochrome b_5 (von Bodman et al., 1986) and myoglobin (Springer & Sligar, 1987), expression of synthetic genes has become a valuable strategy for the efficient production of proteins in heterologous systems. Our findings emphasize the absolute requirement for accuracy in the target amino acid sequence in the successful use of synthetic genes in this manner. Had we not had authentic cytochrome b_5 in hand for direct functional and structural comparison with the original recombinant protein, we would have had no reason to suspect the legitimacy of the recombinant wild-type cytochrome b_5 that we initially produced. Once this discrepancy was discovered and we began to identify the sequence differences between the two proteins, it was only the report of the full-length cDNA sequence for this protein (Cristiano & Steggles, 1989) that eliminated the necessity of redetermining the complete sequence of the authentic protein.

The three-dimensional model of cytochrome b_5 provided by Mathews et al. (1971, 1972) demonstrates that heme propionate-7 forms two hydrogen bonds with Ser-64. One of the carboxylate oxygen atoms forms a hydrogen bond with the serine hydroxyl group while the other forms a hydrogen bond with the Ser-64 main-chain amide group. The model proposed by Argos and Mathews (1975) for the cytochrome b_5 oxidation state change stipulates that these hydrogen-bonding interactions between heme propionate-7 and Ser-64 result in orientation of the heme propionate so that it can help stabilize the net positive charge on the heme iron present in ferricytochrome b_5. In ferrocytochrome b_5, a cation was proposed to bind to heme propionate-7 in a manner that is linked to the change in oxidation state. The results of the present study combined with the model of Argos and Mathews (1975) minimally suggest that the hydrogen bond formed by heme propionate-7 with the main-chain amide group of Ser-64 is sufficient to

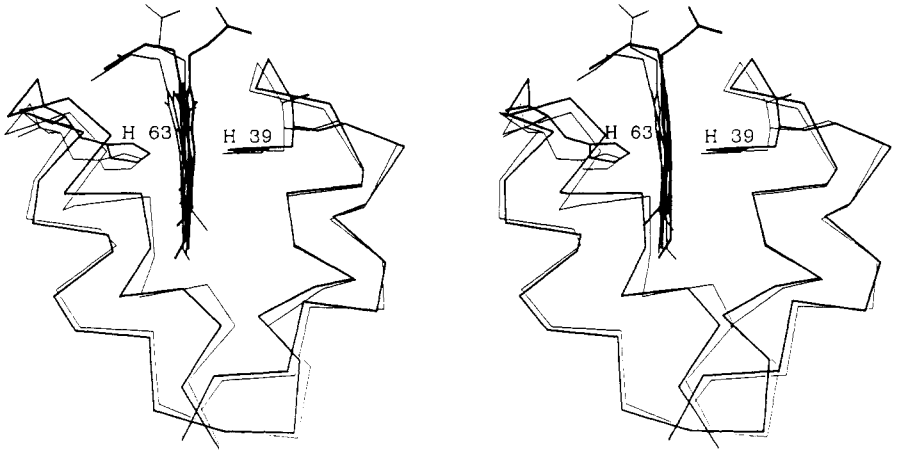

FIGURE 8: Stereo diagram of the wild-type cytochrome b_5 active site region (thin lines) overlayed on the active site region of the triple mutant (thick lines). This view depicts the relative orientations of both heme groups and heme iron ligands.

maintain the heme propionate orientation such that it can adequately stabilize ferricytochrome b_5 to retain the relatively low reduction potential of the wild-type protein. Moreover, insofar as the reduction potential of the Ala-64 mutant is actually several millivolts lower than that of the wild-type protein, this model would argue that elimination of the hydrogen bond between heme propionate-7 and the hydroxyl group of Ser-64 allows the heme propionate to assume an orientation that places the carboxylate group in closer proximity to the heme iron than it is in the wild-type protein.

Interestingly, replacement of the native heme IX with heme IX dimethyl ester produces identical changes in the reduction potentials of both the wild-type cytochrome and the Ala-64 mutant (i.e., they increase by 67 mV). The simplest explanation of this observation is that the reduction potential of the protein is a direct function of the number of charged functional groups in the vicinity of the heme iron. Removal of two charged groups by esterification of the two heme propionate groups thereby raises the reduction potential by an amount corresponding to removal of two negatively charged functional groups. Alternatively, propionate esterification may simply influence the oxidation–reduction equilibrium through elimination of an inductive effect.

The difference in functional properties exhibited by the triple mutant of cytochrome b_5 appears to provide serendipitous insight into other structural considerations that may be important in regulating the reduction potential of cytochrome b_5. On the basis of the structural data discussed above it seems apparent that the lower reduction potential demonstrated by this form of the protein arises from the presence of an aspartyl residue at position 57 rather than an asparaginyl residue. The noninvolvement of substituents at positions 11 and 13 in lowering the reduction potential of the triple mutant has recently been verified by electrochemical measurements of a single-site mutant in which Asn-57 has been changed to Asp-57 that duplicate our findings for the triple mutant (data not shown). This result combined with our observation that elimination of the two heme propionate carboxyl groups (through esterification) increases the potential of the protein by over 60 mV is consistent with the view that the magnitude of carboxylate regulation of the potential is a function of (1) the number of carboxylate groups, (2) their positions with respect to the heme and heme iron, and (3) the dielectric of the medium between the carboxylate(s) and the prosthetic group. By comparing the electrochemical properties of the proteins studied here with those of other derivatives possessing selectively and systematically modified aspartyl and glutamyl residues, it may be possible to ascertain experimentally the dependence of this type of putative Coulombic stabilization on the distance between charged groups. At present, however, these effects cannot be readily separated from the influence of amidation of residue 57 on the position of the heme orientation equilibrium. Notably, Walker et al. (1988) have demonstrated that the reduction potential of cytochrome b_5 is influenced by the orientation of heme binding to the apoprotein in a manner that is comparable in magnitude to the difference in the reduction potentials of the wild-type and triple-mutant cytochromes.

Our conclusion that the mechanistic basis for the difference in electrochemical behavior of the wild-type protein and the triple mutant of cytochrome b_5 constructed on the basis of the originally reported sequence is based on the remarkably small alterations that these three substitutions produce in the three-dimensional structure of the protein. As discussed above, the apparent change in conformation that occurs in the vicinity of Ser-18 can be attributed to differences in crystal packing between the two forms of the protein that result in intermolecular hydrogen-bonding interactions that stabilize an otherwise flexible region of the protein into a single orientation in crystals of the triple-mutant protein. Related observations have been made in crystallization-induced stabilization of otherwise flexible regions of cytochromes c' (Finzel & Salemme, 1985, 1986) and hemerythrins (Sheriff et al., 1985). The conversion of Glu-11 to Gln-11 in the mutant cytochrome b_5 is shown to produce a change in the local environment of His-15 and would be expected to alter its apparent pK_a. We note that the recent report of a discrepancy between the $pK_{1/2}$ predicted for trypsin-solubilized cytochrome b_5 and the $pK_{1/2}$ determined by NMR spectroscopy is probably attributable to the amino acid sequence errors in this region of the protein (Altman et al., 1989). In other words, it is reasonable to expect that inclusion of Glu-11 (rather than Gln-11) in the calculations used to predict the $pK_{1/2}$ for His-15 would result in prediction of a value more in line with the experimentally determined value than was reported. The contribution of the subtle changes in the geometry of the axial ligands to the heme iron in the mutant cytochrome to the electrochemical properties of this protein are difficult to quantify. However, on the basis of the detailed studies of Walker et al. (1988) concerning the quantitative effect of heme orientation and the relatively small perturbation in the axial ligand geometry observed in our mutant, it seems unlikely that the reduction potential would be influenced significantly by this small structural rearrangement.

ACKNOWLEDGMENTS

We thank Tom Atkinson for synthesis of the oligodeoxyribonucleotides, Prof. Ian Clark-Lewis for amino-terminal gas-phase sequence analysis of recombinant cytochrome b_5, Prof. Alan Steggles for communicating the sequence of the bovine liver microsomal cytochrome b_5 cDNA prior to publication, Prof. Scott Mathews and Dr. Rosemary Durley for providing the 1.5 Å resolution wild-type cytochrome b_5 atomic coordinates prior to publication, and Jackie Wilson for assistance in growth of transformed *E. coli*.

REFERENCES

Altman, J., Lipka, J. J., Kuntz, I., & Waskell, L. (1989) *Biochemistry 28*, 7516–7523.

Argos, P., & Mathews, F. S. (1975) *J. Biol. Chem. 250*, 747–751.

Atkinson, T., & Smith, M. (1984) in *Oligonucleotide Synthesis a Practical Approach* (Gait, M. J., Ed.) pp 35–81, IRL Press Ltd., Oxford.

Burch, A. M., Rigby, S. E. J., Funk, W. D., MacGillivray, R. T. A., Mauk, M. R., Mauk, A. G., & Moore, G. R. (1990) *Science 247*, 831–833.

Chaconas, G., & van de Sande, J. H. (1980) *Methods Enzymol. 65*, 75–80.

Connolly, M. L. (1983) *Science 221*, 709–713.

Cristiano, R. J., & Steggles, A. W. (1989) *Nucleic Acids Res. 17*, 799.

Dutton, P. L. (1978) *Methods Enzymol. 54*, 411–435.

Finzel, B. C., & Salemme, F. R. (1985) *Nature (London) 315*, 686–688.

Finzel, B. C., & Salemme, F. R. (1986) *Biophys. J. 49*, 73–76.

Fitzgerald, P. M. D. (1988) *J. Appl. Crystallogr. 21*, 273–278.

Fujinaga, M., & Read, R. J. (1987) *J. Appl. Crystallogr. 20*, 517–521.

Hendrickson, W. A., & Konnert, J. (1981) in *Biomolecular Structure, Function, Conformation and Evolution* (Srinivasan, R., Ed.) Vol. 1, pp 43–57, Pergamon Press, Oxford.

Jakoby, W. B. (1971) *Methods Enzymol. 22*, 248–252.
Keller, R. M., & Wüthrich, K. (1980) *Biochim. Biophys. Acta 621*, 204–217.
Kunkel, T. A. (1985) *Proc. Natl. Acad. Sci. U.S.A. 82*, 488–492.
La Mar, G. N., Toi, H., & Krishnamoorthi, R. (1984) *J. Am. Chem. Soc. 106*, 6395–6401.
Lehninger, A. L. (1970) *Biochemistry*, p 20, Worth Publishers, New York.
Leung, C. J., Nall, B. T., & Brayer, G. D. (1989) *J. Mol. Biol. 206*, 783–785.
Louie, G. V., Hutcheon, W. L. B., & Brayer, G. D. (1988a) *J. Mol. Biol. 199*, 295–314.
Louie, G. V., Pielak, G. J., Smith, M., & Brayer, G. D. (1988b) *Biochemistry 27*, 7870–7876.
Maruyama, T., Gojobori, A. S., & Ikemura, T. (1986) *Nucleic Acids Res. 14*, r151–r197.
Mathews, F. S. (1980) *Biochim. Biophys. Acta 622*, 375–379.
Mathews, F. S. (1985) *Prog. Biophys. Mol. Biol. 45*, 1–56.
Mathews, F. S., & Strittmatter, P. (1969) *J. Mol. Biol. 41*, 295–297.
Mathews, F. S., Argos, P., & Levine, M. (1971) *Cold Spring Harbor Symp. Quant. Biol. 36*, 387–395.
Mathews, F. S., Levine, M., & Argos, P. (1972) *J. Mol. Biol. 64*, 449–464.
McPherson, A. (1982) *Preparation and Analysis of Protein Crystals*, Wiley, New York.
Messing, J. (1983) *Methods Enzymol. 101*, 20–78.
North, A. C. T., Phillips, D. C., & Mathews, F. S. (1968) *Acta Crystallogr., Sect. A 24*, 351–359.
Ozols, J. (1989) *Biochim. Biophys. Acta 997*, 121–130.
Ozols, J. & Strittmatter, P. (1969) *J. Biol. Chem. 244*, 6617–6618.
Pladziewicz, J. R., Meyer, T. J., Broomhead, J. A., & Taube, H. (1973) *Inorg. Chem. 12*, 639–643.
Reid, L. S. (1984) Ph.D. Dissertation, University of British Columbia.
Reid, L. S., & Mauk, A. G. (1982) *J. Am. Chem. Soc. 104*, 841–845.
Reid, L. S., Taniguchi, V. T., Gray, H. B., & Mauk, A. G. (1982) *J. Am. Chem. Soc. 104*, 7516–7519.
Reid, L. S., Mauk, M. R., & Mauk, A. G. (1984) *J. Am. Chem. Soc. 106*, 2182–2185.
Sanger, F., Nicklen, S., & Coulson, A. R. (1977) *Proc. Natl. Acad. Sci. U.S.A. 74*, 5463–5467.
Scherer, G. R. E., Walkinshaw, M. D., Arnot, S., & Morrê, D. J. (1980) *Nucleic Acids Res. 8*, 3895–3907.
Sheriff, S., Hendrickson, W. A., Stenkamp, R. E., Sieker, L. C., & Jensen, L. H. (1985) *Proc. Natl. Acad. Sci. U.S.A. 82*, 1104–1107.
Springer, B. A., & Sligar, S. G. (1987) *Proc. Natl. Acad. Sci. U.S.A. 84*, 8961–8965.
Stormo, G. D., Scheider, T. D., & Gold, L. M. (1982) *Nucleic Acids Res. 10*, 2971–2995.
Strittmatter, P., & Ozols, J. (1966) *J. Biol. Chem. 241*, 4787–4792.
Takano, T., & Dickerson, R. E. (1981a) *J. Mol. Biol. 153*, 79–94.
Takano, T., & Dickerson, R. E. (1981b) *J. Mol. Biol. 153*, 95–115.
Teale, F. W. J. (1959) *Biochim. Biophys. Acta 35*, 543.
Thiessen, W. E., & Levy, H. A. (1973) *J. Appl. Crystallogr. 6*, 309.
von Bodman, S. B., Schuler, M. A., Jollie, D. R., & Sligar, S. G. (1986) *Proc. Natl. Acad. Sci. U.S.A. 83*, 9443–9447.
Walker, F. A., Emrick, D., Rivera, J. E., Hanquet, B. J., & Buttlaire, D. H. (1988) *J. Am. Chem. Soc. 110*, 6234–6240.
Wilson, A. J. C. (1941) *Nature (London) 150*, 151–152.
Zoller, M. J., & Smith, M. (1983) *Methods Enzymol. 100*, 458–500.